Integral membrane proteins Brr6 and Apq12 link assembly of the nuclear pore complex to lipid homeostasis in the endoplasmic reticulum

Christine A. Hodge[1],[*], Vineet Choudhary[2],[*], Michael J. Wolyniak[1],[*],[‡], John J. Scarcelli[1],[§], Roger Schneiter[2],[¶] and Charles N. Cole[1],[3],[¶]

[1]Department of Biochemistry and [3]Department of Genetics, Dartmouth Medical School, Hanover, NH 03755, USA and [2]Division of Biochemistry, Department of Medicine, University of Fribourg, CH-1700 Fribourg, Switzerland

[*]These authors contributed equally to this work
[‡]Present address: Department of Biology, Hampden-Sydney College, Hampden-Sydney, VA 23943, USA
[§]Present address: Tetragenetics, Inc., One Broadway, 14th Floor, Cambridge, MA 02142, USA
[¶]Authors for correspondence (charles.cole@dartmouth.edu; roger.schneiter@unifr.ch)

Summary

Cells of *Saccharomyces cerevisiae* lacking Apq12, a nuclear envelope (NE)-endoplasmic reticulum (ER) integral membrane protein, are defective in assembly of nuclear pore complexes (NPCs), possibly because of defects in regulating membrane fluidity. We identified *BRR6*, which encodes an essential integral membrane protein of the NE-ER, as a dosage suppressor of *apq12Δ*. Cells carrying the temperature-sensitive *brr6-1* allele have been shown to have defects in nucleoporin localization, mRNA metabolism and nuclear transport. Electron microscopy revealed that *brr6-1* cells have gross NE abnormalities and proliferation of the ER. *brr6-1* cells were hypersensitive to compounds that affect membrane biophysical properties and to inhibitors of lipid biosynthetic pathways, and displayed strong genetic interactions with genes encoding non-essential lipid biosynthetic enzymes. Strikingly, *brr6-1* cells accumulated, in or near the NE, elevated levels of the two classes of neutral lipids, steryl esters and triacylglycerols, and over-accumulated sterols when they were provided exogenously. Although neutral lipid synthesis is dispensable in wild-type cells, viability of *brr6-1* cells was fully dependent on neutral lipid production. These data indicate that Brr6 has an essential function in regulating lipid homeostasis in the NE-ER, thereby impacting NPC formation and nucleocytoplasmic transport.

Key words: Membrane dynamics, Nucleocytoplasmic transport, Lipid metabolism, Nucleoporins, Nuclear envelope

Introduction

In eukaryotic cells, all transport between the nucleus and cytoplasm takes place through nuclear pore complexes (NPCs), very large, macromolecular channels that span the inner and outer nuclear membranes (INM and ONM, respectively) (for reviews, see Tran and Wente, 2006, Lim et al., 2008). NPCs have eightfold symmetry perpendicular to the nuclear envelope (NE) and contain multiple copies of approximately 30 proteins called nucleoporins. Relatively little is known about how NPC assembly occurs, which requires fusion of the INM and ONM to create a membrane tunnel within which is embedded an NPC. In metazoan cells, two types of NPC assembly take place: re-assembly late in mitosis as the NE reassembles, and de novo assembly during interphase, when the number of NPCs doubles (for reviews, see Antonin et al., 2008; D'Angelo and Hetzer, 2008). *Saccharomyces cerevisiae* has a closed mitosis and all NPC biogenesis therefore occurs de novo.

Several factors in addition to nucleoporins have been implicated in NPC biogenesis. These include components of the Ran GTPase system (Ryan and Wente, 2002), whose role in coordinating assembly and disassembly of karyopherin-cargo complexes during nucleocytoplasmic transport has been well studied (for reviews, see Conti et al., 2006; Cook et al., 2007; Stewart, 2007; Terry et al., 2007). Cells carrying specific mutant alleles affecting these proteins showed mislocalization of nucleoporins as well as accumulation of nucleoporin-containing cytoplasmic vesicles (Ryan and Wente, 2002; Ryan et al., 2003; Ryan et al., 2007). Proteins involved in endoplasmic reticulum (ER) to Golgi trafficking, including

components of the COPII coat, have also been implicated in NPC assembly (Ryan and Wente, 2002).

Previously, we identified Apq12 in a synthetic genetic array (SGA) screen starting with the *rat8-2* allele of *DBP5*, which encodes a key mRNA export factor (Scarcelli et al., 2007). Apq12 is an integral membrane protein of the ER and NE, and is required for efficient assembly of NPCs (Scarcelli et al., 2007). Although Apq12 is not essential for viability, *apq12Δ* cells are cold sensitive (16°C) for growth and grow best at elevated (>30°C) temperatures. In the absence of Apq12, a subset of nucleoporins mislocalize to cytoplasmic foci, particularly those comprising the cytoplasmic filaments of the NPC. Electron microscopy revealed that *apq12Δ* cells contain many defective pores that contact the INM but not the ONM, where the cytoplasmic filaments are located (Scarcelli et al., 2007).

Addition of the membrane-fluidizing agent benzyl alcohol to *apq12Δ* cells suppressed mislocalization of cytoplasmic filament nucleoporins and defects in mRNA export (Scarcelli et al., 2007). Interestingly, increasing the amount of benzyl alcohol beyond the level used to suppress *apq12Δ* phenotypes causes nucleoporin mislocalization in wild-type cells (Izawa et al., 2004). This suggests that NPC assembly is sensitive to the fluidity of the NE and that the observed defects in NPC assembly in *apq12Δ* cells could result from improper regulation of the lipid composition of the nuclear membrane in response to changes in temperature. Cells respond to changes in temperature and environmental conditions by adjusting the composition of their membranes to maintain the fluidity and

flexibility required for optimal function (Nishida and Murata, 1996). For example, following a shift to lower temperatures, cells adjust the phospholipid composition of their membranes to contain an elevated proportion of unsaturated and shorter acyl chains. Relative levels of other membrane lipid components including sterols also change in response to temperature shifts (Buttke et al., 1980; Sharma, 2006).

To gain further insight into the interplay between biophysical properties of the NE and NPC assembly, we conducted a screen for dosage suppressors of the cold-sensitive growth defect of *apq12Δ*. This screen identified *BRR6*, an essential gene that was originally identified in a screen for cold-sensitive mutants defective in mRNA export (de Bruyn Kops and Guthrie, 2001). Brr6 encodes an integral membrane protein of the ER and NE, with two predicted transmembrane domains. Cells carrying the cold-sensitive *brr6-1* allele are defective for proper localization of some nucleoporins (de Bruyn Kops and Guthrie, 2001). Interestingly, overexpression of *APQ12* partially suppressed the growth defect of *brr6-1* cells, indicating that Apq12 and Brr6 share some common function.

Here, we report that cytoplasmic filaments but not nuclear basket nucleoporins are mislocalized in *brr6-1* cells at low temperatures (16°C-23°C), in a similar fashion to *apq12Δ* cells. In contrast to *apq12Δ*, however, *brr6-1* cells are hypersensitive to agents that increase membrane fluidity such as benzyl alcohol and oleic acid, and to drugs that inhibit sterol or fatty acid synthesis. Consistent with this drug sensitivity, *brr6-1* displays strong genetic interactions with mutants that have defects in the late part of the sterol biosynthetic pathway or in fatty acid elongation. Biochemical analyses revealed that *brr6-1* cells contain dramatically elevated levels of total sterols (particularly steryl esters and episterol) and triacylglycerols (TAGs). Moreover, overproduction of these non-essential storage lipids is functionally important, because *brr6-1* cells are non-viable if neutral lipid synthesis is blocked by deletion of the respective biosynthetic genes. The data indicate that Apq12 and Brr6 are likely to have an important role in regulating lipid homeostasis in the ER, thereby impacting NPC biogenesis, nuclear transport and nuclear mRNA metabolism.

Results

### Genetic interactions between *BRR6* and *APQ12*

To understand better the function of Apq12, we conducted a genetic screen to identify dosage suppressors of the cold-sensitive growth phenotype of *apq12Δ*. We found that high-copy-number plasmids containing *BRR6* restored growth of *apq12Δ* at 16°C to a similar degree as did direct complementation with wild-type *APQ12* (Fig. 1A). Conversely, overexpression of *APQ12* partially suppressed the growth defect of *brr6-1* at both low and high temperatures (Fig. 1A). A double mutant carrying *brr6-1* and *apq12Δ* was unable to grow at all temperatures tested (data not shown). *brr6-1* cells show a modest (30% of cells) mRNA export defect at 30°C, and this was also partially suppressed by overexpression of *APQ12* (Fig. 1B). Interestingly, overexpression of *BRR6* completely suppressed the mRNA export defect of *apq12Δ* cells (Fig. 1B).

To determine whether overexpression of *BRR6* could restore proper localization of nucleoporins in *apq12Δ* cells, we examined the subcellular distribution of GFP-tagged Nup82 and Nup188. Control *apq12Δ* cells carrying an empty vector displayed aberrant localization of both Nup82-GFP and Nup188-GFP, whereas *apq12Δ* cells harboring the *APQ12* plasmid displayed normal nucleoporin
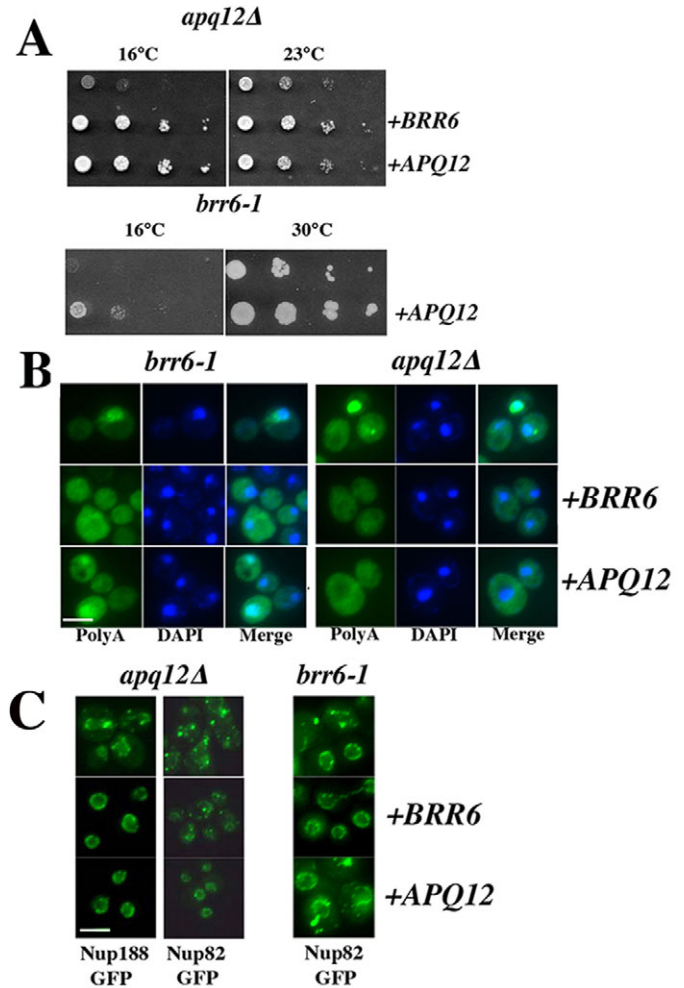
Fig. 1. Dosage suppression of growth, mRNA export and nucleoporin mislocalization of *brr6-1* and *apq12Δ* cells by *APQ12* and *BRR6*. (**A**) Serial dilutions of *apq12Δ* and *brr6-1* cells overexpressing *BRR6* and *APQ12* were spotted onto plates and incubated at the temperatures shown. (**B**) In situ hybridization assay to analyze the effect on the mRNA-export defects of *apq12Δ* and *brr6-1* cells of over-expressing *BRR6* and *APQ12* by using multicopy plasmids. (**C**) Direct visualization of Nup82-GFP and Nup188-GFP in *apq12Δ* and *brr6-1* cells overexpressing *BRR6* and *APQ12*. Nup82-GFP and Nup188-GFP were expressed from the *NUP82* and *NUP188* chromosomal loci. Scale bars: 5 μm.

localization (Fig. 1C). Overexpression of *BRR6* completely restored Nup188-GFP localization, whereas Nup82-GFP localization was partially restored. In the latter case, most cells showed Nup82-GFP at both the NE and in cytoplasmic foci, many of which were located near the nuclear periphery (Fig. 1C, and data not shown). Overexpression of *BRR6* also restored Nup159/Rat7 localization to about the same extent as that of Nup82-GFP (data not shown). Overexpression of *APQ12* partially suppressed mislocalization of nucleoporins in *brr6-1* cells (Fig. 1C). At 30°C and 18°C, the fraction of *brr6-1* cells with mislocalized Nup82-GFP was approximately 25% and 60%, respectively. At 18°C, the fraction was reduced to about 25% in cells overexpressing *APQ1*. Taken together, these results indicate that Apq12 and Brr6 probably have related functions that affect growth at low temperature, mRNA export, and NPC assembly and distribution.
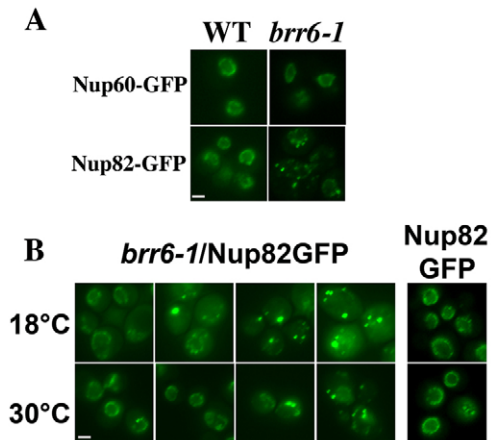
Fig. 2. Mislocalization of cytoplasmic filament nucleoporins in *brr6-1* cells. (**A**) Wild-type and *brr6-1* cells expressing Nup60-GFP or Nup82-GFP were shifted to 20°C overnight and live cells directly visualized. (**B**) Wild-type and *brr6-1* cells grown either at 30°C or shifted to 18°C overnight before visualization. Note the heterogeneity of the distribution of Nup82-GFP in *brr6-1* but not in wild-type cells (right). Scale bars: 5 μm.

brr6-1 affects the assembly of NPC filaments

BRR6 is essential for viability and encodes a 197 amino acid protein; this protein, similarly to Apq12, is an integral membrane protein of the NE-ER, with two predicted transmembrane domains. The *brr6-1* allele (R110K) is both cold (16°C) and heat (37°C) sensitive. However, even at the optimal permissive temperature (30°C), *brr6-1* cells have defects in mRNA export and two core nucleoporins, Nsp1 and Nup188, are mislocalized (de Bruyn Kops and Guthrie, 2001). Because cytoplasmic filaments but not nuclear basket nucleoporins are mislocalized in *apq12Δ* cells (Scarcelli et al., 2007), we extended earlier studies by localizing additional nucleoporins in *brr6-1* cells. This revealed extensive mislocalization

of Nup82-GFP, a cytoplasmic filament nucleoporin, to cytoplasmic and perinuclear foci (Fig. 2A), but no mislocalization of Nup60-GFP, a nuclear basket nucleoporin, at any temperature (data not shown). At all temperatures, Nup82-GFP was localized properly in some cells (with all or most Nup82-GFP at the nuclear periphery), whereas in others, all or most Nup82-GFP was cytoplasmic with many bright foci. Nup159, another cytoplasmic filament nucleoporin, was also extensively mislocalized (data not shown), with phenotypes ranging from normal or nearly normal localization to mislocalization of most or all Nup159-GFP. We hypothesize that the heterogeneity seen in the localization of cytoplasmic filament nucleoporins in the *brr6-1* background reflects the different numbers of copies of plasmid-borne *brr6-1* in different cells. Because we were unable to replace *BRR6* in the genome with *brr6-1*, a single copy of *brr6-1* appears to be insufficient to support growth.

We showed earlier that *apq12Δ* cells are defective in NPC biogenesis but not in NPC stability (Scarcelli et al., 2007) and wanted to determine whether this is also the case for *brr6-1* cells. Two factors complicate this analysis. First, whereas the *apq12Δ* cell population is genetically homogeneous (all cells lack Apq12), *brr6-1* cells are not. The *brr6-1* allele is carried on a *CEN* plasmid (with the genomic copy of *BRR6* deleted), and therefore the number of copies of the mutant gene is not the same in all cells. Second, in *apq12Δ* cells there is no detectable mislocalization of any nucleoporins at 30°C and extensive mislocalization at 16°C (Scarcelli et al., 2007). This makes it straightforward to observe and quantify changes in nucleoporin localization when *apq12Δ* cells are temperature shifted. By contrast, nucleoporins mislocalized in *brr6-1* cells are mislocalized to some extent at all temperatures, although the defect is more severe at lower temperatures. Fig. 2B shows a montage of *brr6-1* cells grown at 30°C or shifted to 18°C overnight. The heterogeneity of phenotypes is readily apparent and indicates that even under optimal growth condition (30°C), Nup82-GFP is mislocalized in many cells. Because cells are able to grow and divide at this temperature, the nucleoporin-mislocalization phenotype indicates that *brr6-1* cells are defective in NPC assembly.
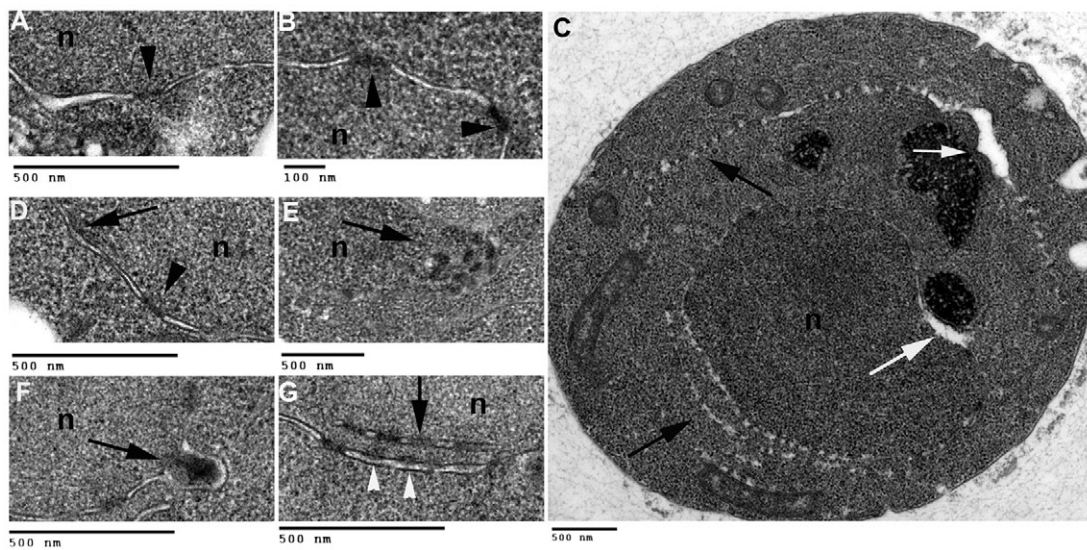

Fig. 3. Electron microscopy reveals NE abnormalities in *brr6-1* cells. Wild-type and *brr6-1* cells were grown at 30°C or shifted to 18°C overnight and processed for thin-section electron microscopy. (**A**) Wild-type cells, 18°C; (**B**) wild-type cells, 30°C; (**C-E**) *brr6-1* cells, 18°C; (**F,G**) *brr6-1* cells, 30°C. Arrows and arrowheads: electron-dense structures and inclusions [arrowheads (A,B,G), arrow (D)], sometimes clustered [arrows (E,F)] or clustered in additional double membranes [black arrows (C,G)]; extensive white expansions of the NE and ER [white arrows (C)]. n, nucleus.

Therefore, it is difficult to determine whether NPCs are also unstable in *brr6-1*.

To define the NPC mislocalization and NE phenotype of *brr6-1* at the ultrastructural level, cells were fixed and analyzed by electron microscopy (Fig. 3). In wild-type cells at both 18°C and 30°C, NPCs appear as electron-dense material that spans the lumen of the NE (arrowhead in Fig. 3A,B). Essentially all NPCs from wild-type cells had this normal appearance. By contrast, in *brr6-1* cells at both 18°C (Fig. 3C-E) and 30°C (Fig. 3F,G) severe abnormalities were seen. The overall number of NPCs or related structures seen in each section was approximately half that seen in wild-type sections. Of these, about one-third appeared to be normal. In *brr6-1* cells, there were many electron-dense inclusions beneath the INM or between the INM and ONM (black arrow in Fig. 3D, white arrowheads in Fig. 3G), often roughly spherical, larger than NPCs and sometimes clustered (arrows in Fig. 3E,F). At 30°C, there were about half as many of these inclusions as normal-appearing NPCs, whereas in cells maintained at 18°C, dense inclusions in these locations were about twice as common as normal-appearing NPCs. Interestingly, membrane blebs, most containing electron-dense inclusions, were seen in *brr6*-1 cells at 30°C (about as many blebs near the NE as there were normal-appearing NPCs), but very rarely in cells maintained at 18°C overnight. We cannot tell whether these are partially-assembled NPCs, aggregates of nucleoporins or other material. In about one-third of thin sections, electron-dense structures were clustered together in additional double-membranes (black arrows in Fig. 3C,G), often extending linearly a considerable distance away from the NE (Fig. 3C). Although these structures resemble NPCs, we do not believe that they are NPCs or NPC-related structures because GFP-tagged nuclear basket nucleoporins and some core nucleoporins were detected only at the nuclear periphery in *brr6-1* cells, and never in these projections (data not shown). The composition of these structures is not known. The extensive white expansions of the NE and ER (white arrows in Fig. 3C) might be lipids, reflecting abnormalities in lipid metabolism (see below). These were observed in approximately 30% of thin sections of *brr6-1* cells, but in only about 5% of sections of wild-type cells, and those seen in wild-type cells were much smaller than those in *brr6-1* cells. In *apq12Δ* cells, there were very few normal NPCs and a large number of what appeared to be partial NPCs extending from the INM part of the way across the lumen of the NE (Scarcelli et al., 2007). Partial NPCs were rare in *brr6-1* cells and very few normal-appearing NPCs were present. This might indicate a more severe NPC assembly defect in these cells compared with *apq12Δ* cells. These aberrant phenotypes were seen very rarely in wild-type cells.

brr6-1 is hypersensitive to treatments that affect membrane fluidity and to drugs that inhibit lipid biosynthesis

A key finding made earlier was that the growth of *apq12Δ* cells in medium containing benzyl alcohol partially suppressed defects in nucleoporin localization and mRNA export (Scarcelli et al., 2007). The growth of *brr6-1* cells was inhibited by benzyl alcohol at all temperatures (Fig. 4A). Since the cold-sensitive phenotype conferred by the *brr6-1* and *apq12Δ* mutations might reflect a loss of ability to make proper adjustments in membrane fluidity, we wondered whether supplementing the medium with the unsaturated fatty acid oleic acid could rescue the defect. Surprisingly, 5 mM oleic acid was detrimental to the growth of both *brr6-1* and *apq12Δ* cells (Fig. 4A).
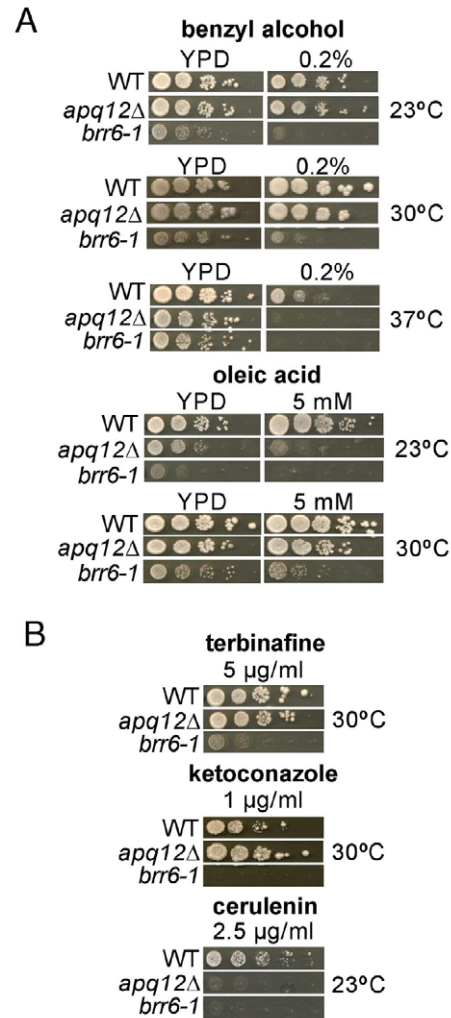
Fig. 4. Effect of compounds that alter membrane properties or inhibit lipid biosynthetic pathways on growth of wild-type, *brr6-1* and *apq12Δ* cells. Serial dilutions of wild-type, *brr6-1* and *apq12Δ* cells were grown on YPD plates or on plates containing: (**A**) the membrane fluidizers benzyl alcohol or oleic acid, or (**B**) drugs that inhibit sterol synthesis (terbinafine and ketoconazole), or fatty acid synthesis (cerulenin) and incubated at the temperatures shown.

We examined the effects on *brr6-1* and *apq12Δ* cells of terbinafine (5-50 μg/ml) and ketoconazole (1-2 μg /ml), which are compounds that inhibit different enzymes in the ergosterol biosynthesis pathway (Petranyi et al., 1984; Sheets and Mason, 1984; Meredith et al., 1985). The two drugs had little or no effect on growth of wild-type or *apq12Δ* cells (Fig. 4B). Strikingly, the *brr6-1* strain was hypersensitive to both. Cerulenin is an inhibitor of fatty acid synthase (Omura, 1981). Growth of both *brr6-1* and *apq12Δ* was inhibited by cerulenin under conditions where growth of wild-type cells was not (Fig. 4B). We conclude that the *brr6-1* mutation confers sensitivity to inhibitors of multiple lipid biosynthetic pathways.

Synthetic genetic interactions between lipid biosynthesis mutants and *brr6-1* and *apq12Δ*

We described earlier the genetic interaction between *apq12Δ* and *acc1-7-1* (Scarcelli et al., 2007). *ACC1* encodes acetyl-CoA

Table 1. Genetic interactions of *apq12Δ* and *brr6-1* with mutations affecting lipid biosynthesis

Lipid mutant tested	Function of encoded protein	*apq12Δ*	*brr6-1*
arv1Δ	Sterol homeostasis, GPI-anchor synthesis	No effect	SL
are1Δ/are2Δ	Acyl-CoA sterol acyltransferases	SS	SL
dga1Δ/lro1Δ	Acyltransferases required for triacylglycerol synthesis	NT	SL
erg2Δ	Ergosterol biosynthesis	SL	SL
erg3Δ	Ergosterolbiosynthesis	No effect	SL
erg4Δ	Ergosterol biosynthesis	No effect	No mating
erg5Δ	Ergosterol biosynthesis	No effect	SL
erg6Δ	Ergosterol biosynthesis	No effect	SL
spo7Δ	Phosphatase as dimer with Nem1p	No effect	SL
nem1Δ	Phosphatase as dimer with Spo7p	SS	No effect
elo1Δ	Fatty acid elongation	No effect	SL
elo2Δ	Fatty acid elongation	No effect	SL
elo3Δ	Fatty acid elongation	No effect	SL
mga2Δ	Transcription factor for *OLE1*	SL	SL
spt23Δ	Transcription factor for *OLE1*	SL	SL

Abbreviations: SL, synthetically lethal; SS, synthetically sick; NT, not tested.

carboxylase, the rate-limiting enzyme in fatty acid synthesis. The *apq12Δ* acc1-7-1 double-mutant strain grew considerably less well than either single mutant at lower temperatures, and considerably better at 34°C than the temperature-sensitive *acc1-7-1* mutant alone. We extended this analysis by testing for synthetic interactions of both *apq12Δ* and *brr6-1* with deletions of non-essential genes whose products act in diverse lipid biosynthetic pathways. The results are summarized in Table 1. *brr6-1* displayed extensive synthetic lethality, with mutations affecting sterol and fatty acid metabolism (e.g. *erg2,erg3,erg5,erg6*; *elo1,elo2,elo3*; *mga2, spt23*). These genetic interactions are consistent with the hypersensitivity of *brr6-1* cells to inhibitors of sterol and fatty acid biosynthesis. Although there were fewer cases where *apq12Δ* showed synthetic lethality or growth defects when combined with lipid biosynthetic mutants, we did observe synthetic growth defects between *apq12Δ* and *erg2Δ*.

Nem1 and Spo7 are subunits of a heterodimeric phosphatase (Siniossoglou et al., 1998; Santos-Rosa et al., 2005) that regulates indirectly several phospholipid biosynthetic genes by modulating the phosphorylation state of Pah1, a transcriptional repressor whose targets are phospholipid biosynthetic genes (Siniossoglou et al., 1998; Santos-Rosa et al., 2005). The morphology of the NE is abnormal in cells lacking Spo7, Nem1 or Pah1/Smp2, which is also the case in *brr6-1* and *apq12Δ* cells. *brr6-1* displayed synthetic lethality with *spo7Δ* but not with *nem1Δ*. This is discussed further below.

apq12Δ and *brr6-1* cells have aberrant lipid profiles

The observations that *brr6-1* and, to a lesser extent, *apq12Δ* cells, are sensitive to drugs that inhibit lipid biosynthetic pathways, together with the fact that these mutants exhibit synthetic interactions with mutations affecting multiple lipid biosynthetic pathways, suggest that Apq12 and Brr6 might directly or indirectly regulate membrane lipid composition and/or lipid synthesis. We examined the phospholipid and neutral lipid composition of *apq12Δ* and *brr6-1* cells by labeling with [³H]palmitic acid for 6 hours at 20, 24 or 37°C. Lipids were extracted and analyzed by thin layer chromatography (TLC). This revealed that wild-type and mutant strains had the same phospholipid composition (data not shown). By contrast, there was a twofold increase in the level of neutral triacylglycerols (TAGs) in *brr6-1* cells at 37°C (Fig. 5A). This hyper-accumulation was rescued completely by the presence of wild-type *BRR6*, indicating that Brr6 function is important for neutral lipid homeostasis at 37°C.

Drug sensitivity and genetic interactions also suggested a possible role for Brr6 in sterol function and/or metabolism. To examine whether *apq12Δ* and *brr6-1* affect sterol metabolism, lipids were
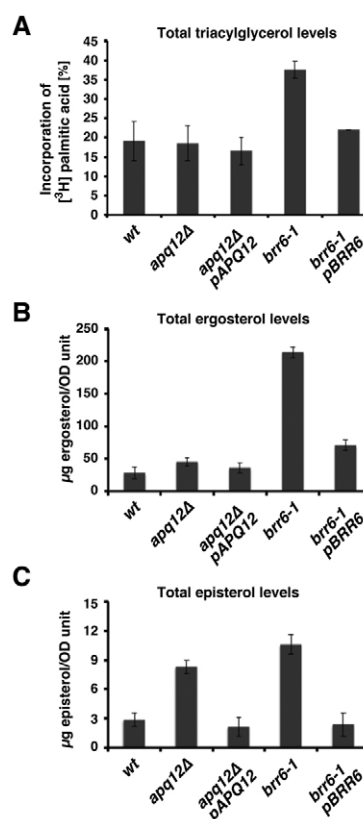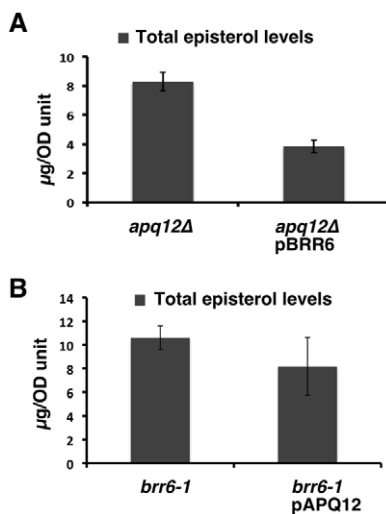

Fig. 5. Analysis of TAGs and sterols in *apq12Δ* and *brr6-1* cells. (A) *brr6-1* cells accumulate triacylglycerols. Cells were labeled with [³H]palmitic acid for 6 hours at 37°C. Lipids were extracted, separated by thin layer chromatography and levels of radiolabeled fatty acids in the different lipid classes were quantified by radio-scanning. (B) *brr6-1* cells have elevated levels of steryl esters. (C) *brr6-1* and *apq12Δ* cells accumulate the sterol precursor episterol. Cells were cultivated overnight at 24°C. Lipids were extracted and sterols were analyzed and quantified by GC-MS, using cholesterol as an internal standard. These analyses were performed independently two (B,C) or three (A) times and results shown are means ± s.e.m.

extracted from cells grown overnight at 24°C, and the sterol profile was determined by gas chromatography and mass spectrometry (GC-MS). This revealed a sevenfold increase in the level of total sterols in *brr6-1* compared with wild-type cells (Fig. 5B), which was due primarily to increased levels of steryl esters, because the levels of free sterols in the *brr6-1* strain were not significantly different from the wild type (data not shown). In addition, this analysis revealed a three- to fourfold increase in the level of the sterol episterol in both *apq12Δ* and *brr6-1* cells (Fig. 5C). Episterol is an intermediate in ergosterol biosynthesis, but is normally present at a very low level. This phenotype was also rescued by the presence of plasmid-borne *APQ12* (in *apq12Δ* cells) or *BRR6* (in *brr6-1* cells). Taken together, these results indicate that *apq12Δ* and *brr6-1* cells have defects in sterol synthesis and that *brr6-1* cells possess a strong defect in neutral lipid homeostasis, resulting in the accumulation of both triacylglycerols and steryl esters.

Overexpression of Brr6 restores normal episterol levels to *apq12Δ* cells

We next tested how the altered sterol levels of *apq12Δ* and *brr6-1* cells were affected by overexpression of *BRR6* or *APQ12*, respectively. The data in Fig. 6A show that overexpression of *BRR6* restored the normal level of episterol in *apq12Δ* cells. By contrast, only a modest reduction in the level of episterol was seen when *APQ12* was overexpressed in *brr6-1* cells (Fig. 6B) and this was not statistically significant. Most likely, the difference in the ability of Apq12 and Brr6 to suppress the defects in episterol levels reflects the fact that Brr6 is essential and Apq12 is not. This could also underlie the partial suppression of the *brr6-1* growth defect by overexpression of *APQ12*, in contrast to the complete suppression of the *apq12Δ* growth defect by *BRR6*. Importantly, the suppression of both the growth defects and elevated episterol level of *apq12Δ* by *BRR6* supports the hypothesis that Apq12 and Brr6 have direct roles in modulating or sensing lipid levels or membrane properties.

Production of neutral lipids is essential for viability of *brr6-1*

To examine whether the increased levels of TAGs and steryl esters in *brr6-1* are of functional importance, we tested the viability of *brr6-1* and *apq12Δ* cells in combination with deletions of *ARE1* and *ARE2*, which encode the two yeast sterol acyltransferases, or *LRO1* and *DGA1,* which encode two acyltransferases that synthesize triacylglycerol. Because an *are1Δ are2Δ* double mutant is viable (Yang et al., 1996; Yu et al., 1996), synthesis of steryl esters is dispensable in an otherwise wild-type background. Similarly, because a *lro1Δ dga1Δ* double mutant is viable, synthesis of triacylglycerides is also dispensable (Oelkers et al., 2002; Sorger and Daum, 2002). However, combining *are1Δ are2Δ* with *brr6-1* caused a strong synthetic growth defect (Fig. 7A), indicating that conversion of free sterols to steryl esters is important for growth of *brr6-1* cells. Synthetic lethality was seen when *brr6-1* was combined with *lro1Δ dga1Δ* (Fig. 7B), indicating that TAG synthesis is essential for growth of *brr6-1* cells.

The fact that *brr6-1* cells accumulate elevated levels of steryl esters and require steryl ester formation for survival could indicate that these cells have elevated levels of free sterols in the ER that might result from a defect in export of free ergosterol from the ER. We monitored the subcellular distribution of sterols using the fluorescent sterol analogue NBD-cholesterol, which we have previously shown to reflect the known natural subcellular distribution of ergosterol (Reiner et al., 2006). Mutant cells deficient in heme production (to block endogenous sterol synthesis and allow uptake of exogenous sterols) were incubated with NBD-cholesterol for 1 hour at 24°C and its distribution was analyzed by fluorescence microscopy. This revealed prominent ring-like staining of the plasma membrane and punctuate intracellular staining of lipid droplets in wild-type cells (Fig. 8A). By contrast, the *brr6-1* mutant displayed substantially elevated staining of aberrantly large lipid droplets that were frequently in close proximity to or possibly associated with the nuclear ER (Fig. 8A, arrowheads), as revealed by visualization of the ER with the ER
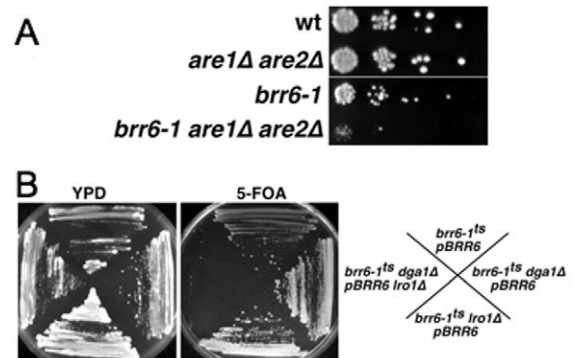

Fig. 6. Overexpression of *BRR6* suppresses the elevated level of episterol in *apq12Δ* cells. *apq12Δ* and *brr6-1* cells containing an empty vector or overexpressing *BRR6* (**A**) or *APQ12* (**B**), respectively, from multicopy plasmids, were cultivated overnight at 24°C. Lipids were extracted and sterols were analyzed and quantified by GC-MS. These analyses were performed independently two times and results shown are means ± s.e.m.

Fig. 7. Production of steryl esters and triacylglycerides is essential in *brr6-1* cells. (**A**) Analysis of *brr6-1* synthetic interactions with *are1Δ are2Δ*. *ARE1* and *ARE2* were deleted in a *brr6-1* background to produce the *are1Δ are2Δ brr6-1* triple mutant. Growth of the indicated strains on YPD plates is shown. (**B**) Analysis of *brr6-1* synthetic interactions with *lro1Δ dga1Δ*. *LRO1* and *DGA1* were deleted in a *brr6-1* strain containing a wild-type copy of *BRR6* on a *URA3* plasmid. Cells were plated on YPD plates and then replicated to YPD plates and to plates containing 5-fluoro-orotic acid (5-FOA) to select for colonies that have lost the *URA3 BRR6* plasmid. Plates were incubated for 4 days at 24°C.

luminal marker Kar2-mRFP-HDEL (Gao et al., 2005). Endogenously produced sterols showed similar localization, as revealed by staining with filipin (data not shown). Lipid droplets are dedicated storage organelles for neutral lipids and contain primarily steryl esters and triacylglycerides. These observations, together with the observed elevated levels of steryl esters, indicate that *brr6-1* hyperesterifies sterols that are synthesized endogenously, as well as sterols taken up from the outside.

To monitor the sterol hyperesterification phenotype more directly, heme-deficient cells were incubated with [^{14}C]cholesterol and the conversion of free cholesterol to steryl esters was analyzed by TLC analysis of radiolabeled sterols. This revealed that *brr6-1* cells accumulated approximately one-third more free sterol (Fig. 8B) than wild-type cells. Furthermore, *brr6-1* cells had a strongly elevated rate of steryl ester formation as they produced three times as many

steryl esters than wild-type cells after 8 hours of incubation in medium containing [^{14}C]cholesterol (Fig. 8B).

The observation that *brr6-1* has strongly elevated levels of the two neutral lipids, steryl esters and TAGs, and the fact that steryl ester and TAG formation is essential in *brr6-1* point to a possible function of Brr6 in neutral lipid homeostasis. The enzymes that synthesize neutral lipids (Are1, Are2, Dga1 and Lro1) are localized in ER membranes (for a review, see Czabany et al., 2007). The resulting neutral lipids are then deposited into lipid droplets. These lipid droplets are believed to be formed from the ER membrane, from which they might bud off to become independent organelles (Murphy and Vance, 1999). It is interesting to note that *apq12Δ* was identified as an *mld* (many lipid droplets) mutant in a screen of the yeast knockout strains to identify mutants with altered lipid-droplet morphology (Fei et al., 2008).

To examine whether *brr6-1* displayed an aberrant lipid-droplet phenotype, lipid droplets were visualized using Erg6-RFP as a marker protein. Erg6-RFP was mislocalized to the NE in *brr6-1* cells, and lipid droplets were frequently seen encircling the NE of these cells (Fig. 9, arrowheads). Quantification of this lipid droplet phenotype revealed that in 72.5% of *brr6-1* cells, lipid droplets were arranged in a circular pattern around the DAPI-stained nucleus. In wild-type or *apq12Δ* cells, by contrast, lipid droplets were observed in a circular pattern around the nucleus in fewer than 30% of cells. These observations suggest that the overproduction of neutral lipids in *brr6-1* results in over-accumulation of neutral lipids in the NE and perinuclear ER, where the enzymes for TAG and steryl ester synthesis are located, and that these neutral lipids are not efficiently partitioned into lipid droplets. Accumulation of neutral lipids in the ER, as suggested by ultrastructural analysis (Fig. 3C), could then result in altered membrane properties and defects in NPC assembly.
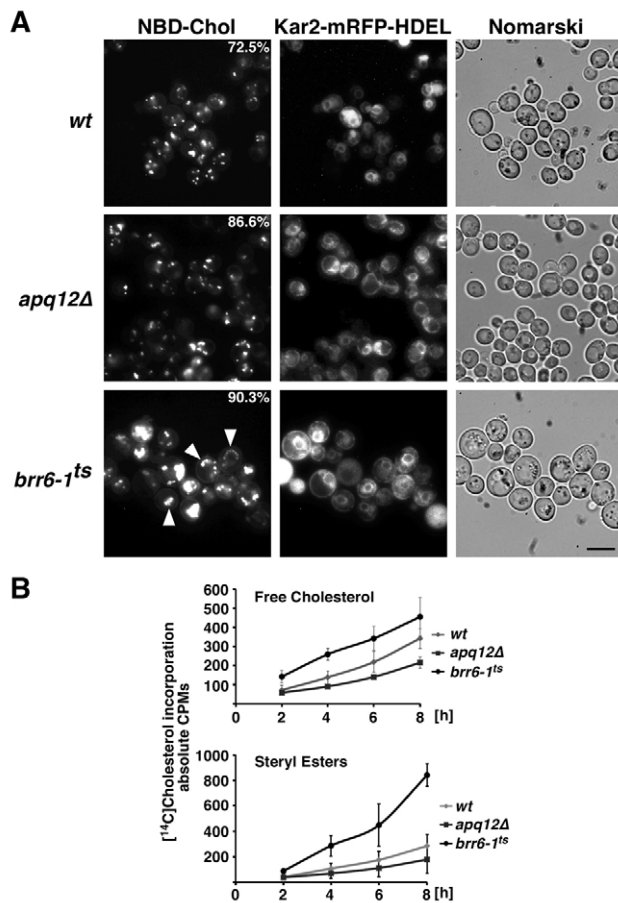
Fig. 8. *brr6-1* cells accumulate free sterols and steryl esters. (A) Subcellular distribution of NBD-cholesterol. Heme-deficient cells of the indicated genotype and expressing the ER marker Kar2-mRFP-HDEL were incubated with the fluorescent sterol analog NBD-cholesterol for 1 hour at 24°C and the distribution of NBD-cholesterol was analyzed by fluorescence microscopy. White arrowheads indicate staining of the NE-ER. The numbers indicate the proportion of NBD-cholesterol-stained lipid droplets that colocalize with the Kar2-mRFP-HDEL-stained NE-ER (*n*=100 cells). Scale bar: 5 μm. (B) Heme-deficient cells of the indicated genotype were incubated with [^{14}C]cholesterol. Samples were removed at the time points indicated, lipids were extracted and the levels of free and esterified cholesterol were quantified. Results shown are means ± s.e.m.
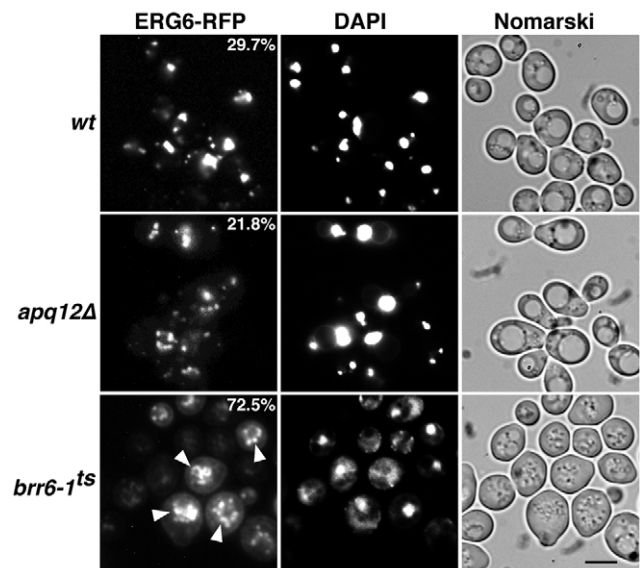
Fig. 9. *brr6-1* cells have aberrant lipid droplets. Cells were transformed with a plasmid expressing the lipid droplet marker protein Erg6-RFP and analyzed by fluorescence microscopy. White arrowheads indicate lipid droplets that encircle the NE-ER. The numbers indicate the proportion of cells that display circular arrangement of Erg6-RFP marked lipid droplets around the nucleus (*n*=100 cells). DNA was revealed by staining with DAPI. Scale bar: 5 μm.

Discussion

Genetic interactions and similar mutant phenotypes for *brr6-1* and *apq12Δ*

We identified *BRR6* as a dosage suppressor of *apq12Δ*. *brr6-1* and *apq12Δ* are synthetically lethal, and *APQ12* and *BRR6* were able to suppress the cold-sensitive growth defects of each other (Fig. 1). Although the phenotypes seen in *brr6-1* cells are similar to those of *apq12Δ*, *brr6-1* defects were generally much stronger. *brr6-1* was more sensitive to chemical and pharmacological agents that impact lipid biosynthesis and membrane fluidity, showed more extensive alterations in the levels of neutral lipids, and was synthetically lethal with more lipid biosynthetic mutants than was *apq12Δ*. These differences are consistent with a more important role for Brr6 in the maintenance of membrane fluidity, than for Apq12, which is not essential.

A third gene, encoding a Brr6-related protein, *BRL1* (*BRR6*-like), was identified as a suppressor of a temperature-sensitive *xpo1* (exportin 1) mutant (Saitoh et al., 2005). Brl1 is essential, has substantial homology to Brr6 (24% identical and 46% similar) and is also found in the NE. Proteins containing the domain shared between Brr6 and Brl1 are present in fungi that undergo closed mitoses, including *Candida glabarata* and *Cryptococcus neoformans*. *brl1* mutants share phenotypes of nucleoporin mislocalization and mRNA-export defects with *brr6-1* and *apq12Δ* (Saitoh et al., 2005). *BRR6* was able to suppress the growth defect of *brl1* mutants, which were synthetically lethal with *brr6-1*. Brl1 and Brr6 interacted with each other in a two-hybrid analysis (Saitoh et al., 2005). However, we found that *BRL1* could not suppress *apq12Δ* (unpublished results). Future studies will investigate the possibility that these three proteins function together.

Normal nuclear morphology is dependent upon membrane composition

Many earlier studies indicated that the shape of the nucleus is related to lipid composition of cellular membranes. Nem1 and Spo7 are the catalytic and regulatory subunits, respectively, of an ER-NE-associated protein phosphatase (Siniossoglou et al., 1998; Santos-Rosa et al., 2005). The target of this enzyme is Pah1/Smp2 (Santos-Rosa et al., 2005), which acts as a transcriptional repressor of several phospholipid biosynthesis genes and is a homologue of mammalian Lipin, expressed at a high level in adipose tissue (Peterfy et al., 2001). Pah1 has phosphatidic acid phosphatase activity and thereby controls the synthesis of triacylglycerols (Han et al., 2006). *NEM1*, *SPO7* and *PAH1* are non essential, but strains lacking any one have abnormal nuclear morphology including extensions of the NE that contain NPCs (Siniossoglou et al., 1998; Tange et al., 2002). Overproduction of Pah1 restores normal nuclear membrane structure to *nem1Δ* and *spo7Δ* cells. In cells lacking Pah1, defects in lipid metabolism affect multiple classes of lipids including triacylglycerols (Han et al., 2006). These studies demonstrate that nuclear shape and the distribution of NPCs depends upon proper regulation of lipid biosynthesis. The finding that *brr6-1* is synthetically lethal with *spo7Δ* but not *nem1Δ* suggests that deletions of *NEM1* and *SPO7* affect certain aspects of TAG synthesis differently from each other. Spo7 is the regulatory subunit for the Spo7/Nem1 heterodimer (Siniossoglou et al., 1998; Santos-Rosa et al., 2005) and could be important for localized activation of Pah1. This might explain why *brr6-1* is lethal when combined with *spo7Δ* but viable when combined with *nem1Δ*. We also found that *PAH1* is essential in our wild-type strain background. *PAH1*, *SPO7* and *NEM1* have also been linked genetically to *NUP84*

(Siniossoglou et al., 1998; Santos-Rosa et al., 2005). Together, these results are consistent with our finding that *apq12Δ* and *brr6-1* cells have alterations in lipid metabolism, NE structure and shape, and nucleoporin localization.

Other studies have suggested that the lipid composition of NE itself is important for NPC biogenesis. A mutation in *ACC1/MTR7*, which encodes acetyl CoA carboxylase, was isolated in a screen for mRNA-export mutants (Schneiter et al., 1996). Acc1 is essential, and is responsible for synthesis of malonyl CoA, the key building block for synthesis of fatty acids. *mtr7-1 acc1-7-1* cells have been shown to have abnormal NPCs and mislocalized nucleoporins, and were defective in the formation of very-long-chain fatty acids, something not observed with other *acc1* alleles (Schneiter et al., 1996). This suggested that very-long-chain fatty acids might have a role in NPC assembly, perhaps by helping to bring together the INM and ONM at points where fusion is to occur, as NPCs are assembled (Schneiter et al., 1996; Schneiter et al., 2004).

brr6-1 and *apq12Δ* might affect the functioning of a membrane-fluidity sensor

An interesting possibility to account for our results is that the *apq12Δ* and *brr6-1* mutations impact the known ability of cells to sense environmental changes that normally trigger modifications in membrane composition needed to maintain membrane homeostasis (for reviews, see Murata and Los, 1997; Los and Murata, 2004; Zhang and Rock, 2008). Little is known about how fluidity and other biophysical properties of membranes are sensed and how this information is transduced to adjust lipid synthesis and membrane composition. Fluidity sensors are thought to respond to decreases in temperature, in part through activating fatty acid desaturases, which introduce double-bonds into acyl chains of fatty acids and phospholipids, and thereby have a large impact on the melting temperature of membranes. To function properly, cells must be able to sense the need to induce changes in membrane composition and to prevent changes of too great a magnitude.

Yeast has a single fatty acid desaturase, Ole1 (Stukey et al., 1989), whose production is tightly regulated. Mga2 and Spt23, two homologous membrane-associated transcription factors related to mammalian NF-κB, are released from membrane association by proteolysis when cells sense the need to activate *OLE1* (Hoppe et al., 2000). Neither Mga1 nor Spt23 is essential, but cells lacking both are not viable (Zhang et al., 1999). *brr6-1* showed synthetic lethality with both *mga2Δ* and *spt23Δ* (Table 1). Morphological defects in the NE were seen following a shift of an *mga2Δ spt23-ts* mutant to non-permissive temperature (Zhang et al., 1999). Cells lacking Ole1 are able to grow when supplemented with unsaturated fatty acids (UFAs) but the membrane abnormalities seen following depletion of UFAs are substantially more severe than those seen in *mga2Δ spt23-ts* cells (Zhang et al., 1999). One possibility to account for this is that membrane anchoring of Mga2 and Spt23 might be sensitive to changes in membrane fluidity, such that changes in fluidity could promote proteolytic activation of Mga2 and Spt23, thereby leading to inappropriate activation of *OLE1*.

If *brr6-1* or *apq12Δ* cells were defective in their ability to induce modifications in membrane composition in response to a shift to a lower temperature, it might be expected that supplementing the medium with oleic acid would at least partially suppress the defects. The double bond in the oleate acyl chain introduces a kink that disrupts acyl chain packing in the lipid bilayer. An increase in oleate incorporation into phospholipids therefore can

increase membrane fluidity (Hazel, 1995). Suppression of *brr6-1* and *apq12Δ* by oleic acid was not observed. Rather, both strains showed sensitivity to oleic acid at 23°C and *brr6-1* cells were also sensitive to oleic acid at 30°C (Fig. 4A). This suggests that the observed defects might reflect an excess of membrane fluidity at lower temperatures, as opposed to a deficit, which is consistent with the hypersensitivity of *brr6-1* cells to benzyl alcohol. If this were the case, then the primary defect might be the inability of cells to sense when proper membrane composition and dynamics had been restored following a temperature shift.

Lipid esterification is essential for viability of *brr6-1* mutant cells

Our finding that the viability of *brr6-1* cells depends on esterification of sterols (Fig. 7) is particularly intriguing and suggests that these cells accumulate elevated levels of free sterols in the ER that need to be neutralized by esterification so that they do not adversely affect ER and NE function. Elevated levels of free cholesterol in the ER of animal cells result in depletion of ER calcium stores, induction of the unfolded protein response (UPR) and ultimately apoptosis (Feng et al., 2003). Mechanistically, this has been explained by an inhibition of the normal conformational freedom of ER by the cholesterol-induced increase in membrane lipid order (Li et al., 2004). In yeast, Arv1, which is a conserved ER integral membrane protein, is required for viability of cells that cannot esterify free sterols. Previous work has shown that *arv1Δ* mutant cells accumulate sterols in the ER and display elevated levels of steryl esters (Tinkelenberg et al., 2000). Arv1 is also required for the maturation of glycosylphosphatidylinositol (GPI) anchors, which are attached to the C-terminus of proteins in the ER lumen. The alterations in sphingolipid and sterol levels observed in *arv1Δ* have been proposed to be a secondary consequence of a reduced flux of lipids out of the ER (Swain et al., 2002; Kajiwara et al., 2008). Our observation that *arv1Δ* is synthetically lethal with *brr6-1* indicates that Brr6 provides an overlapping function with Arv1 required for lipid homeostasis in the ER. Although we did not observe defects in ER function in *apq12Δ* cells (Scarcelli et al., 2007), growth of *brr6-1* is sensitive to tunicamycin (our unpublished results), a characteristic of mutants with defects in ER function.

Because *brr6-1* cells contain elevated levels of TAGs and steryl esters, they would be expected to be more resistant to cerulenin than wild-type cells are. Fatty acids can be released from TAGs and steryl esters to bypass and compensate for the block in fatty acid synthesis caused by cerulenin. Because *brr6-1* cells are more sensitive than the wild type to cerulenin, they appear to depend more strongly on ongoing fatty acid synthesis. This might be needed to move another lipid (free sterol, diacylglycerol, or phosphatidic acid) into the neutral lipid pool, where any excess would be less harmful than in a non-acylated form. The finding that *brr6-1* is synthetically lethal with *elo1Δ, elo2Δ* and *elo3Δ*, supports the idea that the ability to make a range of fatty acids has increased importance when cells are mutant for *brr6*.

The data presented here provide strong support for the hypothesis that Apq12 and Brr6 have a direct role in lipid and membrane homeostasis and that the observed defects in NPC biogenesis and mRNA export are consequences of the resulting altered membrane properties. Because many strains with defects in mRNA export (e.g. *rat8-2/dbp5, mex67-5, prp20-1*) have normal NPCs and NE (Aebi et al., 1990; Segref et al., 1997; Tseng et al., 1998), an mRNA-export defect cannot be the underlying cause of the NE and lipid metabolism abnormalities seen in *apq12Δ* and *brr6-1* cells. Defects

in NPCs and the NE are seen in some strains that lack a non-essential nucleoporin or produce a mutant form of an essential nucleoporin. This might indicate that unsuccessful attempts to assemble NPCs can lead to defects in the NE, perhaps resulting from abnormal interactions between the NE and integral membrane nucleoporins or nucleoporins that have a role in curvature of the NE at sites of NPC insertion. However, the fact that neither Apq12 nor Brr6 are components of NPCs makes it unlikely that the primary direct defect from mutations affecting these proteins is in NPC assembly. It will be interesting to see whether there are defects in lipid metabolism in these nucleoporin mutant strains.

It is striking that the NE and NPC defects seen in *brr6-1* and *apq12Δ* cells are considerably more severe than in cells lacking individual non-essential lipid metabolism genes or those treated with a range of compounds that affect membrane properties and lipid biosynthesis. Further studies will be required to understand the mechanism by which Brr6 and Apq12 affect lipid metabolism and the fluidity of the nuclear membrane, and how this impacts NPC biogenesis.

Materials and Methods

Yeast strains and plasmids
The strains and plasmids used in these studies are listed in supplementary material Table S1. All strains were grown and media prepared using standard methods (Sambrook et al., 1989). For growth assays, strains were grown overnight, then diluted back to $OD_{600}=0.3$. Strains were then serially diluted 1:10, and 3 μl of each dilution was plated.

Microscopy
Live-cell fluorescence microscopy was performed using cells grown and mounted in SCD medium. Images were acquired using a Nikon TE2000-E microscope fitted with a Nikon ×100 Plan Apochromat oil objective (NA 1.4), Orca-ER CCD camera (Hamamatsu, Bridgewater, NJ) and Phylum Live Software, version 3.5.1 (Improvision, Lexington, MA) or a Zeiss Axioplan 2 microscope (Carl Zeiss, Oberkochen, Germany) equipped with an AxioCam CCD camera and AxioVision 3.1 software. GFP, Cy3 and Cy5 were visualized by using an X-cite 120 UV lamp and Chroma filter sets. Images were processed using Adobe Photoshop (Adobe Systems, San Jose CA). The fluorescence in situ hybridization assay (FISH) was performed as described previously (Cole et al., 2002).

Electron microscopy
Electron microscopy was performed as previously described (Scarcelli et al., 2007). In brief, the cells were grown to an OD_{600} of 0.5-1.0 in YPD medium, pelleted and resuspended in 0.1 M cacodylate buffer, pH 6.8. Primary fixation was performed with 3% glutaraldehyde, 1% paraformaldehyde and 0.1% tannic acid in 0.1 M cacodylate buffer, pH 6.8, at room temperature for 1 hour and then overnight at 4°C. Cells were washed twice with 0.1 M cacodylate buffer, pH 6.8, and twice with 0.1 M phosphate buffer, pH 7.5, and treated with zymolyase 100T (10 mg/ml) to produce spheroplasts. After washing with phosphate buffer, pH 7.5, and cacodylate buffer, pH 6.8, the cells were retreated with 3% glutaraldehyde, 1% paraformaldehyde and 0.1% tannic acid in 0.1 M cacodylate buffer, pH 6.8, for 1 hour at room temperature, washed three times with 0.1 M cacodylate buffer, pH 6.8, and embedded in low melting temperature agarose (SeaPrep; FMC). Post fixation was performed with 2% osmium tetroxide in 0.1 M cacodylate buffer, pH 6.8, for 1 hour on ice. Subsequently, the cells were washed in cacodylate buffer, pH 6.8, and deionized water, en bloc stained with 0.5% uranyl acetate overnight, dehydrated with ethanol, and embedded in Spurr's resin (medium grade). Thin sections were cut on an ultramicrotome (MT5000; Sorvall) with a section thickness of 100 nm. Sections were poststained with uranyl acetate and Venable and Coggleshell's lead citrate and examined on a transmission electron microscope (JEM 1010; JEOL) at 100 kV.

High-copy *apq12Δ* suppressor screen
A Yep13 2 μ *LEU2* library (Rose and Broach, 1991) was utilized to identify genes that could suppress *apq12Δ* cold-sensitivity at 16°C. The library was transformed into *apq12Δ* cells, and cells were plated on leucine dropout medium and incubated at 16°C for 14 days. Candidate suppressor colonies were retested for growth at 16°C. *apq12Δ* cells carrying an empty *LEU2* vector were included as a negative control.

Drug treatment
All compounds were purchased from Sigma and dissolved in dimethyl sulfoxide (DMSO) prior to addition to media. Terbinafine from Neil Ryder (Novartis Research Institute, Vienna, Austria) was used in some experiments. With the exception of oleic acid and palmitic acid, the appropriate compound was added to YPD medium

following autoclaving. Oleic acid and palmitic acid were added before autoclaving along with 0.5% Tween-40 to facilitate dissolving. Compounds were used at the following concentrations: 0.2% benzyl alcohol, 5 mM oleic acid, 5 µg/ml terbinafine, 1 µg/ml ketoconazole, 2.5 µg/ml cerulenin. For growth analysis in the presence of these agents, strains were diluted tenfold four times across rows of a 96-well plate, and 4 µl samples from the original and diluted samples were spotted onto YPD plates supplemented with the appropriate agent. Plates were grown for 5 days at 23°C, 30°C and 37°C and photographed after 3 and 5 days or at 16°C for 14 days and photographed after 7 and 14 days.

Lipid analysis

Total lipids were analyzed following [^{3}H]palmitic acid labeling of cells. Cells were cultivated in YPD at 24°C, diluted in fresh medium and incubated at 20°C, 24°C or 37°C for 1 hour before addition of 10 µCi/ml of [9,10-^{3}H]palmitic acid (10 mCi/ml; American Radiolabeled Chemicals, St Louis, MO). After 6 hours of labeling, cells were collected, lipids were extracted with chloroform and methanol (1:1, v/v), lipids were dried under a stream of nitrogen and aliquots of the lipid extract containing equal counts were analyzed by thin layer chromatography (TLC) using silica gel 60 plates (Merck, Darmstadt, Germany). Phospholipids were separated using the solvent system chloroform, methanol and potassium-chloride (0.25%) (55:45:5, v/v/v). Neutral lipids were separated using petroleum ether, diethyl ether and glacial acetic acid (70:30:2, v/v/v). Plates were then analyzed by radio-TLC scanning (Tracemaster 20, Berthold Technologies, Bad Wildbad, Germany) and exposure to a phosphorimaging screen (Bio-Rad).

For sterol analysis, cells were cultivated in SC medium overnight at 24°C and processed essentially as described (Quail and Kelly, 1996) using cholesterol as internal standard. Free sterols and base-hydrolyzed total sterols were derivatized by TMS [N′O′-bis-(trimethylsilyl)-trifluoroacetamide] and analyzed by GC-MS on a Voyager Trace 2000 Series GC-MS (Thermo Fisher Scientific, Waltham, MA) equipped with a Zebron ZB-35 capillary column (35% phenyl-methyl polysiloxane; dimensions: 30 m × 0.25 mm × 0.25 µm film thickness). Sterols were identified based on their mass fragmentation pattern and by comparison to commercially available standards. Staining cells with NBD-cholesterol, sterol uptake and esterification were performed as previously described (Reiner et al., 2006).

Supplementary material available online at
http://jcs.biologists.org/cgi/content/full/123/1/141/DC1

References

Aebi, M., Clark, M. W., Vijayraghavan, U. and Abelson, J. (1990). A yeast mutant, PRP20, altered in mRNA metabolism and maintenance of the nuclear structure, is defective in a gene homologous to the human gene RCC1 which is involved in the control of chromosome condensation. *Mol. Gen. Genet.* **224**, 72-80.

Antonin, W., Ellenberg, J. and Dultz, E. (2008). Nuclear pore complex assembly through the cell cycle: regulation and membrane organization. *FEBS Lett.* **582**, 2004-2016.

Buttke, T. M., Jones, S. D. and Bloch, K. (1980). Effect of sterol side chains on growth and membrane fatty acid composition of *Saccharomyces cerevisiae*. *J. Bacteriol.* **144**, 124-130.

Cole, C. N., Heath, C. V., Hodge, C. A., Hammell, C. M. and Amberg, D. C. (2002). Analysis of RNA export. *Methods Enzymol.* **351**, 568-587.

Conti, E., Muller, C. W. and Stewart, M. (2006). Karyopherin flexibility in nucleocytoplasmic transport. *Curr. Opin. Struct. Biol.* **16**, 237-244.

Cook, A., Bono, F., Jinek, M. and Conti, E. (2007). Structural biology of nucleocytoplasmic transport. *Annu. Rev. Biochem.* **76**, 647-671.

Czabany, T., Athenstaedt, K. and Daum, G. (2007). Synthesis, storage and degradation of neutral lipids in yeast. *Biochim. Biophys. Acta.* **1771**, 299-309.

D'Angelo, M. A. and Hetzer, M. W. (2008). Structure, dynamics and function of nuclear pore complexes. *Trends Cell Biol.* **18**, 456-466.

de Bruyn Kops, A. and Guthrie, C. (2001). An essential nuclear envelope integral membrane protein, Brr6p, required for nuclear transport. *EMBO J.* **20**, 4183-4193.

Fei, W., Shui, G., Gaeta, B., Du, X., Kuerschner, L., Li, P., Brown, A. J., Wenk, M. R., Parton, R. G. and Yang, H. (2008). Fld1p, a functional homologue of human seipin, regulates the size of lipid droplets in yeast. *J. Cell Biol.* **180**, 473-482.

Feng, B., Yao, P. M., Li, Y., Devlin, C. M., Zhang, D., Harding, H. P., Sweeney, M., Rong, J. X., Kuriakose, G., Fisher, E. A. et al. (2003). The endoplasmic reticulum is the site of cholesterol-induced cytotoxicity in macrophages. *Nat. Cell Biol.* **5**, 781-792.

Gao, X. D., Tachikawa, H., Sato, T., Jigami, Y. and Dean, N. (2005). Alg14 recruits Alg13 to the cytoplasmic face of the endoplasmic reticulum to form a novel bipartite UDP-N-acetylglucosamine transferase required for the second step of N-linked glycosylation. *J. Biol. Chem.* **280**, 36254-36262.

Gorsch, L. C., Dockendorff, T. C. and Cole, C. N. (1995). A conditional allele of the novel repeat-containing yeast nucleoporin RAT7/NUP159 causes both rapid cessation of mRNA export and reversible clustering of nuclear pore complexes. *J. Cell Biol.* **129**, 939-955.

Han, G. S., Wu, W. I. and Carman, G. M. (2006). The *Saccharomyces cerevisiae* Lipin homolog is a Mg2+-dependent phosphatidate phosphatase enzyme. *J. Biol. Chem.* **281**, 9210-9218.

Hazel, J. R. (1995). Thermal adaptation in biological membranes: is homeoviscous adaptation the explanation? *Annu. Rev. Physiol.* **57**, 19-42.

Hoppe, T., Matuschewski, K., Rape, M., Schlenker, S., Ulrich, H. D. and Jentsch, S. (2000). Activation of a membrane-bound transcription factor by regulated ubiquitin/proteasome-dependent processing. *Cell* **102**, 577-586.

Izawa, S., Takemura, R. and Inoue, Y. (2004). Gle2p is essential to induce adaptation of the export of bulk poly(A)+ mRNA to heat shock in *Saccharomyces cerevisiae. J. Biol. Chem.* **279**, 35469-35478.

Kajiwara, K., Watanabe, R., Pichler, H., Ihara, K., Murakami, S., Riezman, H. and Funato, K. (2008). Yeast *ARV1* is required for efficient delivery of an early GPI intermediate to the first mannosyltransferase during GPI assembly and controls lipid flow from the endoplasmic reticulum. *Mol. Biol. Cell* **19**, 2069-2082.

Li, Y., Ge, M., Ciani, L., Kuriakose, G., Westover, E. J., Dura, M., Covey, D. F., Freed, J. H., Maxfield, F. R., Lytton, J. et al. (2004). Enrichment of endoplasmic reticulum with cholesterol inhibits sarcoplasmic-endoplasmic reticulum calcium ATPase-2b activity in parallel with increased order of membrane lipids: implications for depletion of endoplasmic reticulum calcium stores and apoptosis in cholesterol-loaded macrophages. *J. Biol. Chem.* **279**, 37030-37039.

Lim, R. Y., Ullman, K. S. and Fahrenkrog, B. (2008). Biology and biophysics of the nuclear pore complex and its components. *Int. Rev. Cell Mol. Biol.* **267**, 299-342.

Los, D. A. and Murata, N. (2004). Membrane fluidity and its roles in the perception of environmental signals. *Biochim. Biophys. Acta* **1666**, 142-157.

Meredith, C. G., Maldonado, A. L. and Speeg, K. V., Jr (1985). The effect of ketoconazole on hepatic oxidative drug metabolism in the rat in vivo and in vitro. *Drug Metab. Dispos.* **13**, 156-162.

Murata, N. and Los, D. A. (1997). Membrane fluidity and temperature perception. *Plant Physiol.* **115**, 875-879.

Murphy, D. J. and Vance, J. (1999). Mechanisms of lipid-body formation. *Trends Biochem. Sci.* **24**, 109-115.

Nishida, I. and Murata, N. (1996). Chilling sensitivity in plants and cyanobacteria: The crucial contribution of membrane lipids. *Annu. Rev. Plant Physiol. Plant Mol. Biol.* **47**, 541-568.

Oelkers, P., Cromley, D., Padamsee, M., Billheimer, J. T. and Sturley, S. L. (2002). The DGA1 gene determines a second triglyceride synthetic pathway in yeast. *J. Biol. Chem.* **277**, 8877-8881.

Omura, S. (1981). Cerulenin. *Methods Enzymol.* **72**, 520-532.

Peterfy, M., Phan, J., Xu, P. and Reue, K. (2001). Lipodystrophy in the *fld* mouse results from mutation of a new gene encoding a nuclear protein, lipin. *Nat. Genet.* **27**, 121-124.

Petranyi, G., Ryder, N. S. and Stutz, A. (1984). Allylamine derivatives: new class of synthetic antifungal agents inhibiting fungal squalene epoxidase. *Science* **224**, 1239-1241.

Quail, M. A. and Kelly, S. L. (1996). The extraction and analysis of sterols from yeast. *Methods Mol. Biol.* **53**, 123-131.

Reiner, S., Micolod, D., Zellnig, G. and Schneiter, R. (2006). A genomewide screen reveals a role of mitochondria in anaerobic uptake of sterols in yeast. *Mol. Biol. Cell* **17**, 90-103.

Rose, M. D. and Broach, J. R. (1991). Cloning genes by complementation in yeast. *Methods Enzymol.* **194**, 195-230.

Ryan, K. J. and Wente, S. R. (2002). Isolation and characterization of new *Saccharomyces cerevisiae* mutants perturbed in nuclear pore complex assembly. *BMC Genet.* **3**, 17.

Ryan, K. J., McCaffery, J. M. and Wente, S. R. (2003). The Ran GTPase cycle is required for yeast nuclear pore complex assembly. *J. Cell Biol.* **160**, 1041-1053.

Ryan, K. J., Zhou, Y. and Wente, S. R. (2007). The karyopherin Kap95 regulates nuclear pore complex assembly into intact nuclear envelopes *in vivo. Mol. Biol. Cell* **18**, 886-898.

Saitoh, Y. H., Ogawa, K. and Nishimoto, T. (2005). Brl1p - a novel nuclear envelope protein required for nuclear transport. *Traffic* **6**, 502-517.

Sambrook, J., Fritsch, E. F. and Maniatis, T. (1989). Molecular Cloning: a Laboratory Manual. Cold Spring Harbor, NY: Cold Spring Harbor Laboratory.

Santos-Rosa, H., Leung, J., Grimsey, N., Peak-Chew, S. and Siniossoglou, S. (2005). The yeast lipin Smp2 couples phospholipid biosynthesis to nuclear membrane growth. *EMBO J.* **24**, 1931-1941.

Scarcelli, J. J., Hodge, C. A. and Cole, C. N. (2007). The yeast integral membrane protein Apq12 potentially links membrane dynamics to assembly of nuclear pore complexes. *J. Cell Biol.* **178**, 799-812.

Schneiter, R., Hitomi, M., Ivessa, A. S., Fasch, E. V., Kohlwein, S. D. and Tartakoff, A. M. (1996). A yeast acetyl coenzyme A carboxylase mutant links very-long-chain fatty acid synthesis to the structure and function of the nuclear membrane-pore complex. *Mol. Cell. Biol.* **16**, 7161-7172.

Schneiter, R., Brugger, B., Amann, C. M., Prestwich, G. D., Epand, R. F., Zellnig, G., Wieland, F. T. and Epand, R. M. (2004). Identification and biophysical characterization

of a very long-chain-fatty-acid-substituted phosphatidylinositol in yeast subcellular membranes. *Biochem. J.* **381**, 941-949.

Segref, A., Sharma, K., Doye, V., Hellwig, A., Huber, J., Luhrmann, R. and Hurt, E. (1997). Mex67p, a novel factor for nuclear mRNA export, binds to both poly(A)+ RNA and nuclear pores. *EMBO J.* **16**, 3256-3271.

Sharma, S. C. (2006). Implications of sterol structure for membrane lipid composition, fluidity and phospholipid asymmetry in *Saccharomyces cerevisiae*. *FEMS Yeast Res.* **6**, 1047-1051.

Sheets, J. J. and Mason, J. I. (1984). Ketoconazole: a potent inhibitor of cytochrome P-450 dependent drug metabolism in rat liver. *Drug Metab. Dispos.* **12**, 603-606.

Siniossoglou, S., Santos-Rosa, H., Rappsilber, J., Mann, M. and Hurt, E. (1998). A novel complex of membrane proteins required for formation of a spherical nucleus. *EMBO J.* **17**, 6449-6464.

Sorger, D. and Daum, G. (2002). Synthesis of triacylglycerols by the acyl-coenzyme A:diacyl glycerol acyltransferase Dga1p in lipid particles of the yeast Saccharomyces cerevisiae. *J. Bacteriol.* **184**, 519-524.

Stewart, M. (2007). Molecular mechanism of the nuclear protein import cycle. *Nat. Rev. Mol. Cell. Biol.* **8**, 195-208.

Stukey, J. E., McDonough, V. M. and Martin, C. E. (1989). Isolation and characterization of *OLE1*, a gene affecting fatty acid desaturation from *Saccharomyces cerevisiae*. *J. Biol. Chem.* **264**, 16537-16544.

Swain, E., Stukey, J., McDonough, V., Germann, M., Liu, Y., Sturley, S. L. and Nickels, J. T., Jr (2002). Yeast cells lacking the *ARV1* gene harbor defects in sphingolipid metabolism. Complementation by human *ARV1*. *J. Biol. Chem.* **277**, 36152-36160.

Tange, Y., Hirata, A. and Niwa, O. (2002). An evolutionarily conserved fission yeast protein, Ned1, implicated in normal nuclear morphology and chromosome stability, interacts with Dis3, Pim1/RCC1 and an essential nucleoporin. *J. Cell Sci.* **115**, 4375-4385.

Terry, L. J., Shows, E. B. and Wente, S. R. (2007). Crossing the nuclear envelope: hierarchical regulation of nucleocytoplasmic transport. *Science* **318**, 1412-1416.

Tinkelenberg, A. H., Liu, Y., Alcantara, F., Khan, S., Guo, Z., Bard, M. and Sturley, S. L. (2000). Mutations in yeast *ARV1* alter intracellular sterol distribution and are complemented by human *ARV1*. *J. Biol. Chem.* **275**, 40667-40670.

Tran, E. J. and Wente, S. R. (2006). Dynamic nuclear pore complexes: life on the edge. *Cell* **125**, 1041-1053.

Tseng, S. S., Weaver, P. L., Liu, Y., Hitomi, M., Tartakoff, A. M. and Chang, T. H. (1998). Dbp5p, a cytosolic RNA helicase, is required for poly(A)+ RNA export. *EMBO J.* **17**, 2651-2662.

Winston, F., Dollard, C. and Ricupero-Hovasse, S. L. (1995). Construction of a set of convenient *Saccharomyces cerevisiae* strains that are isogenic to S288C. *Yeast* **11**, 53-55.

Yang, H., Bard, M., Bruner, D. A., Gleeson, A., Deckelbaum, R. J., Aljinovic, G., Pohl, T. M., Rothstein, R. and Sturley, S. L. (1996). Sterol esterification in yeast: a two-gene process. *Science* **272**, 1353-1356.

Yu, C., Kennedy, N. J., Chang, C. C. and Rothblatt, J. A. (1996). Molecular cloning and characterization of two isoforms of Saccharomyces cerevisiae acyl-CoA:sterol acyltransferase. *J. Biol. Chem.* **271**, 24157-24163.

Zhang, S., Skalsky, Y. and Garfinkel, D. J. (1999). *MGA2* or *SPT23* is required for transcription of the delta9 fatty acid desaturase gene, *OLE1*, and nuclear membrane integrity in *Saccharomyces cerevisiae*. *Genetics* **151**, 473-483.

Zhang, Y. M. and Rock, C. O. (2008). Membrane lipid homeostasis in bacteria. *Nat. Rev. Microbiol.* **6**, 222-233.

Table S1. Strains and plasmids used in this study

Strain name	Relevant genotype	Source
FY23	*MATa trp1Δ63 leu2Δ1 ura3-52*	(Winston et al., 1995)
BY4742 (wt)	*MATα his3 ura3Δ0 leu2Δ0 lys2*	Research Genetics
APQ12-GFP	*MATa his3 ura3Δ0 leuΔ0 met15Δ0 APQ12-GFP::kan^R*	Invitrogen
apq12Δ	*MATα his3 ura3Δ0 leu2Δ0 lys2 APQ12::KAN^R*	Research Genetics
arv1Δ	*MATa his3 ura3Δ0 leu2Δ0 lys2 Avr1::KAN^R*	Research Genetics
erg2Δ	*MATa his3 ura3Δ0 leu2Δ0 lys2 Erg2::KAN^R*	Research Genetics
erg3Δ	*MATa his3 ura3Δ0 leu2Δ0 lys2 Erg3::KAN^R*	Research Genetics
erg4Δ	*MATa his3 ura3Δ0 leu2Δ0 lys2 Erg4::KAN^R*	Research Genetics
erg5Δ	*MATa his3 ura3Δ0 leu2Δ0 lys2 Erg5::KAN^R*	Research Genetics
erg6Δ	*MATa his3 ura3Δ0 leu2Δ0 lys2 Erg6::KAN^R*	Research Genetics
elo1Δ	*MATa his3 ura3Δ0 leu2Δ0 lys2 Elo1::KAN^R*	Research Genetics
elo2Δ	*MATa his3 ura3Δ0 leu2Δ0 lys2 Elo2::KAN^R*	Research Genetics
elo3Δ	*MATa his3 ura3Δ0 leu2Δ0 lys2 Elo3::KAN^R*	Research Genetics
spo7Δ	*MATa his3 ura3Δ0 leu2Δ0 lys2 Spo7::KAN^R*	Research Genetics
spo14Δ	*MATa his3 ura3Δ0 leu2Δ0 lys2 Spo14::KAN^R*	Research Genetics
nem1Δ	*MATa his3 ura3Δ0 leu2Δ0 lys2 Nem1::KAN^R*	Research Genetics
mga2Δ	*MATa his3 ura3Δ0 leu2Δ0 lys2 MGA2::KAN^R*	Research Genetics
spt23Δ	*MATa his3 ura3Δ0 leu2Δ0 lys2 SPT23::KAN^R*	Research Genetics
LGY103	*MATa rat7-1 his3_200 ura3-52 leu2_1*	(Gorsch et al., 1995)
CHY244	*M A T a rat7ΔN his3_200 ura3-52 leu2_1trp1Δ63*	(Scarcelli et al., 2007)
CSY538	*his3-200 leu 2Δ0 ura3-53 brr6::His NUP82-GFP::kan^R pBRR6 (URA CEN)*	This study
CSY539	*his3-200 leu 2Δ0 ura3-53 brr6::His NUP60-GFP::kan^R pBRR6 (URA CEN)*	This study

Nup60-GFP	*MATα his3 ura3Δ0 leuΔ0 met15Δ0 NUP60-GFP::kan^R*	Invitrogen
Nup82-GFP	*MATα his3 ura3Δ0 leuΔ0 met15Δ0 NUP82-GFP::kan^R*	Invitrogen
RSY3018	*MATα his3Δ1 leu2Δ0 lys2Δ0 ura3Δ0 met15Δ0 trp1Δ are1::kan^R are2::kan^R*	This study
RSY3552	*MATα his3Δ1 leu2Δ0 lys2Δ0 ura3Δ0 hem1::LEU2 apq12:: kan^R*	This study
RSY3786	*MATα ade2-1 ura3-1 his3-11,15 trp1-1 leu2-3,112 hem1::TRP1 brr6::HIS3/brr6-1(LEU2*	This study
RSY2033	*MATα his3Δ1 leu2Δ0 lys2Δ0 ura3Δ0 hem1::LEU2*	(Reiner et al., 2006)
RSY3785	*MATα ade2-1 ura3-1 his3-11,15 trp1-1 leu2-3,112 brr6::HIS3/brr6-1(LEU2) are1::LoxP are2::LoxP*	This study
RSY4186	*MATα ade2-1 ura3-1 his3-11,15 trp1-1 leu2-3,112 brr6::HIS3/brr6-1(LEU2) pBRR6 (2μm, URA3) lro1:: kan^R*	This study
RSY4183	*MATα ade2-1 ura3-1 his3-11,15 trp1-1 leu2-3,112 brr6::HIS3/brr6-1(LEU2) pBRR6 (2μm, URA3) lro1:: kan^R dga1::loxP*	This study
RSY4185	*MATα ade2-1 ura3-1 his3-11,15 trp1-1 leu2-3,112 brr6::HIS3/brr6-1(LEU2) pBRR6 (2μm, URA3) dga1::loxP*	This study
yDBK166	*MATα ade2-1 ura3-1 his3-11,15 trp1-1 leu2-3,112 brr6::HIS3/brr6-1(LEU2)*	(de Bruyn Kops and Guthrie, 2001)
JSy050	*his3 ura3Δ0 leu2Δ0 NUP82-GFP::HIS3 apq12::KAN^R*	(Scarcelli et al., 2007)
JSy068	*his3 ura3Δ0 leu2Δ0 NUP188-GFP::HIS3 apq12::KAN^R*	(Scarcelli et al., 2007)
MWY1	*MATα his3_200 ura3-52 leu2_1 trp1Δ63 BRR6::HIS3 pBRR6 (URA3/CEN)*	This study
MWY2	*MATα his3_200 ura3-52 leu2_1trp1Δ63 BRR6::HIS3 pbrr6-1 (LEU2/CEN)*	This study
Plasmid name	**Description**	**Source**
p*APQ12*	YEplac195 (2μm, *URA3*) with *APQ12*	This study
p*BRR6*	YEplac195 (2μm, *URA3*) with *BRR6*	This study
p*brr6-1*	YCplac111 (*LEU2/CEN*) brr6-1	This study
pERG6-RFP	*pGREG506 (URA3/CEN) with ERG6-RFP*	This study
pHDEL-RFP	*pGREG506 (URA3/CEN) with HDEL-RFP*	This study